

VOLUME TEN

DEVELOPMENTS IN VOLCANOLOGY

CALDERA VOLCANISM: ANALYSIS, MODELLING AND RESPONSE

Editors

JOACHIM GOTTSMANN

*Department of Earth Sciences,
University of Bristol,
Bristol, United Kingdom*

JOAN MARTÍ

*Institute of Earth Sciences,
CSIC, Lluís Sole Sabaris s/n,
Barcelona, Spain*



ELSEVIER

Amsterdam • Boston • Heidelberg • London • New York • Oxford
Paris • San Diego • San Francisco • Singapore • Sydney • Tokyo

FACILITATING DIKE INTRUSIONS INTO RING-FAULTS

Thomas R. Walter*

Contents

1. Introduction	352
2. Modeling Method	355
3. Results	356
3.1. Deformation around a depressurized magma chamber	356
3.2. Predicting the location of ring-dike intrusions	359
3.3. How processes external to the caldera system may affect the location of ring-dike intrusions	363
4. Discussion	367
5. Conclusion	371
Acknowledgements	371
References	371

Abstract

Most caldera volcanoes are associated with circular dike intrusions. Ring-dikes form during complete or partial subsidence of the caldera floor and may be responsible for eruption locations that surround a structural basin. Through a systematic set of numerical models, this paper summarizes a variety of types, mechanisms, and patterns of caldera ring-dikes that can be observed in nature. Caldera subsidence is simulated by magma chamber depressurization; three main sets of models are distinguished. First, local linear and circular faults are included in order to understand their effect on caldera-related displacements. Second, passive opening at a ring-fault is studied in order to understand where ring-dike intrusions may occur. Third, models are designed to exemplify how processes external to the caldera, such as a tectonic earthquake or an eccentric intrusion, may affect the location of a ring-dike intrusion. These models suggest that ring-dikes commonly form “incompletely,” i.e. only part of a ring can be intruded because of the nonuniform displacement field around the ring-fault. As described in the discussion, these models help explain the locations of ring-dikes in various volcanic regions.

*Corresponding author. Tel.: +49 (0)331 288 1253; Fax: +49 (0)331 288 1204
E-mail address: twalter@gfz-potsdam.de

GFZ Potsdam, Telegrafenberg, 14473 Potsdam, Germany

1. INTRODUCTION

Large-volume ash-flow eruptions and sporadic cones typically align along the circumference of a caldera basin (e.g., Walker, 1984; Lipman, 1997; Cole et al., 2005). Studies of caldera structures show that groups of eruption feeder pathways form discordant intrusive bodies with near-circular geometries in map view. Intrusions along a circle around a volcanic center were described in detail in the early twentieth century (Clough et al., 1909); these intrusions are referred to as *ring-complexes*. Ring-complexes are very common for volcanoes with surface expressed calderas (Richey, 1935; Smith and Bailey, 1968; Lipman, 1984), and different types are distinguished. The geometry of ring-complexes comprise circular or angular, inwardly dipping, vertical, and outwardly dipping dikes of variable thickness. These can be singular intrusion events or multiple dikes, forming basaltic or silicic sheets. Intrusion dynamics of ring-complexes include those that generate their own propagating fractures or those that reactivate existing fracture zones. In the latter case, the dike may follow predefined faults of regional tectonic and/or volcano-tectonic origin.

In association with collapsed calderas, two main types of ring-complexes can be distinguished (see Table 1): inwardly dipping (often 30–45°) concentric dikes, referred to as cone sheets (Bailey et al., 1924), and near-vertical or often outwardly dipping concentric dikes intruded parallel to (or into) the ring-faults, referred to as ring-dikes (Anderson, 1936; Billings, 1943). In the mid-1930s, E.M. Anderson developed the first mathematical theory for the development of ring-complexes (Anderson, 1936); a fluctuating pressure within a deep parabolic magma chamber is thought to be responsible for the formation of ring-complexes. The two different types of ring-complexes are therefore defined geometrically as well as genetically; while cone sheets are thought to form during stages of caldera floor uplift (inflation), ring-dikes form during stages of caldera floor subsidence (deflation). This work focuses on the different conditions and geometries of ring-dike formation related to caldera subsidence.

Ring-dikes ideally intrude along the ring-fault and form a closed ring; more commonly, they only partially intrude into a ring-fracture to form curved or segmented dikes (Billings, 1943; Bonin, 1986). Ring-dikes are often only a few centimeters or meters thick. However, old eroded caldera system ring-dikes can reach massive dimensions, wider than 10 km and more than 0.5 km thick. Classic ring-dikes were described for volcanic systems in Scotland; for instance, at Glencoe caldera, a deeply eroded caldera with inverted relief, caldera subsidence affects an oval-shaped area and activated boundary faults (Clough et al., 1909). Although similar mechanisms were applied to most intrusive complexes in the British Volcanic Tertiary Province (Richey, 1935), newer studies suggest that some of these ring-complexes are lopolithic intrusions associated with inflation and doming (O'Driscoll et al., 2006).

A major difficulty in ring-dike studies is that exposures are usually poor and often obscured by sedimentary caldera infill or other intrusive bodies (O'Driscoll et al., 2006; Kennedy and Stix, 2007). It has been shown that the geometry of a

Table 1 Classification of ring-complexes into cone sheets and ring dykes.

Domain	Class	Geometry				Genetics	Composition	Timing	Structural control
		Dip	Strike	Width	Number				
Ring complex	Cone sheets	Inward dip, 30–45° multiple sheets	Mainly circular or elliptical	Scale cm to m	Multiple intrusions, sheets	Forceful dyke intrusion from an over-pressurised reservoir	Mainly evolved magmas	Late stages, resurgence	Little
	Ring dykes	Vertical to outward dip, >90° often single event only	Circular, elliptical, angular, polygonal	Scale m to km	Often individual dykes	May also intrude passively into opening (ring) faults	All kinds, primitive to evolved magmas	All stages, before, during, or after caldera formation	Major

ring-fault is important for ring-dikes. Based on studies using field constraints (Newhall and Dzurisin, 1988), laboratory work (Komuro, 1987; Roche et al., 2000; Acocella et al., 2001; Walter and Troll, 2001; Kennedy and Stix, 2003; Geyer et al., 2006) and numerical modeling (Komuro et al., 1984; Gudmundsson, 1988; Burov and Guillou Frottier, 1999; Kusumoto and Takemura, 2003, 2005), it now appears that ring-fault location, dip, and slip are mainly controlled by the depth and geometry of the magma chamber. The depth of a magma chamber is usually between 2 and 15 km. For example, an intrusive body is suspected to be 2 km beneath the Yellowstone caldera, 4–7 km beneath the Long Valley caldera, and 5–15 km beneath the Valles caldera (Lipman, 1997). Calderas are often elliptical, for instance the 35×73 km Garita caldera, and the presently active Rabaul caldera, which is 5×10 km. Besides such geometrical difficulties, combinations of stress fields, for instance, those due to a second deep magma chamber or regional tectonics, may influence the geometries of ring-complexes near the surface (Marti et al., 1996; Gudmundsson, 1998). In order to understand the general formation and appearance of ring-faults, the reader is referred to other papers within this volume detailing the structural development of caldera-related fault structures.

Ring-faults are often described as pure dip-slip structures; however, as shown by the conceptual model of Figure 1 and by the abundance of intrusive dikes along these faults, ring-faults (re)activate as opening mode fractures (Anderson, 1936). The necessary space for ring-dike intrusion can be generated during caldera floor subsidence. In fact, many former ring-faults are used as dike propagation paths, such that outcrops of ring-dikes appear to be more common than outcrops of ring-faults. A caldera ring-fault may become active during magma pressure changes associated with, for example, input of fresh magma from deeper sources (Sparks et al., 1984) or magma evacuation (Druitt and Sparks, 1984). Also, caldera ring-faults may slip or open due to tectonic activity, a remote stress field, or pre-existing strain history (Gudmundsson, 1988; Newhall and Dzurisin, 1988; Marti et al., 2000;

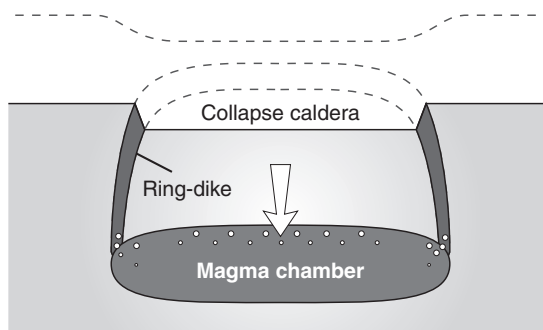


Figure 1 Sketch of ring-dike formation. During deflation of a large magma chamber (decrease of magma pressure), the chamber roof subsides (white arrow) to form subvertical or outwardly dipping ring-faults. A ring-dike (shown in dark gray) intrudes into such ring-faults. The ring-dike may reach the surface, as shown here, or may occur only underground and develop a bell-jar geometry and the surface flexure above (this geometry is shown by the dashed lines).

Bosworth et al., 2003), and thereby influence ring-dike intrusions. This means that ring-dikes may be emplaced in association with both magma chamber pressure changes and extrinsic processes. In this paper, the conditions under which ring-fractures may open to facilitate ring-dikes will be further explored and summarized. This work uses a set of boundary element models that address the question of where and under which circumstances a ring-fracture is subject to opening, and thus examines the geometric possibility of ring-dikes. The first models are simple, using spherical magma chambers and cylindrical ring-fractures. More complex models are then designed in order to understand the effects of ellipsoidal and sill-shaped chambers, and to test how extrinsic activities, such as peripheral radial dikes or earthquakes, can affect the locations and patterns of subsequent ring-dikes. Natural ring-dikes strongly compare to the patterns described herein (see Section 4). This paper intends to provide a general overview of ring-dike formation using numerical models, with the goal of stimulating successive studies at key locations elsewhere.

2. MODELING METHOD

Numerical models are performed in a three-dimensional linear elastic half-space medium, using a boundary element code (Crouch and Starfield, 1983; Becker, 1992; Thomas, 1993). The modeling method is based on the analytical solutions for angular dislocations in isotropic half- and full space (Comninou and Dundurs, 1975), and has already been used in various studies concerning the development of stress in volcanoes (e.g., Walter et al., 2005; Walter and Amelung, 2006). Using combinations of angular dislocations, polygonal (triangular) boundary elements are made that together can describe complex three-dimensional objects. This allows finite magma chambers and ring-faults of various dimensions to be considered. Boundary conditions are defined as tractions or displacements at the center of each element. Linear equations are solved in order to calculate displacement distributions along faults, dikes, and magma chambers. For a more detailed description, see Thomas (1993).

This study considers (i) a deflating magma chamber of various geometries (spherical, oblate spheroid, ellipsoid), (ii) a subvertical ring-fault surrounding the magma chamber (spherical, elliptical), (iii) freely slipping faults that may be reactivated during magma chamber evacuation, and (iv) dike intrusion and faulting in the periphery of the ring-fault.

The boundary element method was validated by comparing it with the analytical solution of a spheroid source (Yang et al., 1988); results agree within a few percentage for the studied range of geometries. The type of loading as shown in this paper is pressure change at the magma chamber by -10 MPa (depressurization). If other types of loading were applied, they are specified below. A Young's modulus of $E = 70$ GPa and a Poisson's ratio of $\nu = 0.25$ were assigned that were typical values for the shallow crust (Turcotte and Schubert, 2002). Varying these material properties can affect the magnitude of the results, but the patterns remain similar.

Various model geometries were considered, and tests were conducted for reservoir radii of 5 and 10 km, yielding very similar results. For spherical chambers, a radius of 5 km was used, while for elliptical chambers, 10×5 km was chosen. These diameters agree with most known calderas (Newhall and Dzurisin, 1988). The depth chosen for the chambers was 10 km to the reservoir center, thus between 5 and 7.5 km to the reservoir roof. Although realistic loading conditions and geometries were applied for all models, the results are used mainly in a qualitative way. The main goal of these model simulations is to emphasize the geometric complexities of ring-dikes at various caldera systems.

3. RESULTS

Three main sets of results are distinguished. First, deformation around a depressurized magma chamber is described together with how local structures can affect deformation. Second, the amount a ring-fault surrounding the depressurized magma chamber opens is described in order to examine the potential locations of dike intrusions. Third, models are designed to exemplify how processes external to the caldera, such as an earthquake or intrusion, can affect the location of a ring-dike intrusion. The results are shown in map view, cross-section, and side views as displacement vectors and contour plots. A coordinate system is indicated in each of the figures for orientation; x - y is used for the horizontal plane and z denotes the vertical direction, so a view in the x - z plane is a side view.

3.1. Deformation around a depressurized magma chamber

3.1.1. Deflating spherical magma chamber

First, a simple scenario with a deflating magma chamber embedded in a uniform elastic material is considered. The magma chamber is spherical, with a radius $r = 5$ km, located at a depth $d = 10$ km below the surface (i.e. the depth of the roof of the chamber is 5 km). The magma chamber is subjected to a pressure drop of 10 MPa; this is the only type of loading in these models. The model setup is shown in Figure 2A, and results are shown in map view (Figure 2B) and along a cross-section west to east (x - x' , Figure 2C, D). The horizontal displacement field, shown by displacement vectors, indicates movement of the material towards the deflating source. Contours in Figure 2B indicate the amount of vertical displacement (U_z), which is negative and thus defines subsidence. The cross-sections indicate the horizontal displacement field (U_x , Figure 2C), showing that the material on the west side of the chamber is displaced to the east, while the material on the east of the chamber is displaced to the west (Figure 2D). At the surface, the maximum horizontal displacement occurs at a slightly eccentric location above the edge of the chamber. The vertical displacement field (U_z) shows that the material above the chamber sinks downward (Figure 2D); maximum subsidence occurs in a bell-shaped area just above the magma chamber. Below the chamber, a slight upward

Deflating spherical magma reservoir

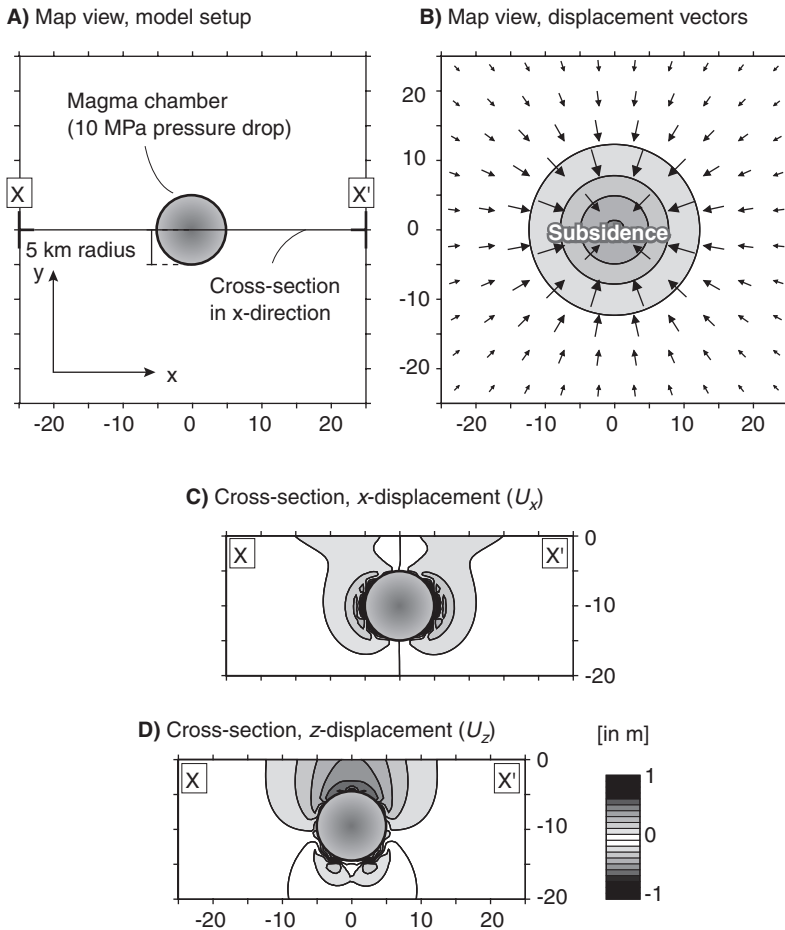


Figure 2 Deflation of a spherical magma chamber. (A) Map view of model setup (x – y plane). The magma chamber (5 km radius) is emplaced at (x, y) coordinates (0, 0) at 10 km depth, and is subject to a pressure drop of 10 MPa. (B) Map view of displacement vectors at the surface (x – y plane). The vectors converge toward the deflating source. Contours indicate negative vertical displacement (subsidence). (C) Cross-section x – x' . The displacement field in the horizontal direction (U_x) shows peak values near the chamber and at two locations at the surface. (D) Cross-section x – x' . The displacement field in the vertical direction (U_z) shows a bell-shaped subsidence area.

displacement can be observed (Figure 2D). Similar models have been studied by other researchers in order to simulate, for example, caldera formation, elastic flexure due to (under) pressurized sources, and related surface deformation (Gudmundsson, 1988, 1999; Bosworth et al., 2003; Kusumoto and Takemura, 2003; Pinel and Jaupart, 2005; Dzurisin, 2007).

3.1.2. Deflating spherical magma chamber with a nearby reactivated fault

Caldera systems are often located in tectonic areas already faulted by previous geological processes. In this set of models, a fault is introduced that is passively allowed to slip in the along-strike and dip-slip direction. All other model parameters, magma chamber shape and position, loading and output, are the same as described in the previous model. The fault is vertical and oriented south to north, 5 km from the magma chamber (Figure 3A). Displacements are calculated in map view (Figure 3B) and along cross-section $x-x'$, perpendicular to the fault (Figure 3C, D). The pattern of subsidence above the evacuating magma chamber

Deflating spherical magma reservoir nearby reactivated fault

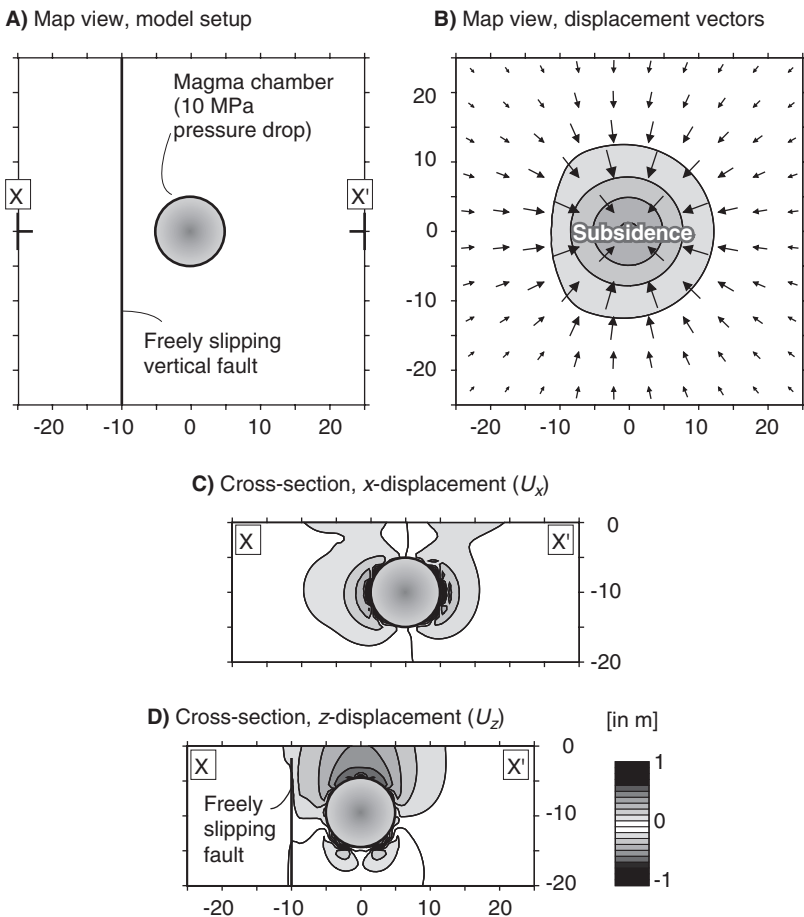


Figure 3 Deflation of a spherical magma chamber near a reactivated fault. (A) Model setup ($x-y$ plane). A linear vertical fault is defined 10 km from the magma chamber, from 2 to 20 km depth. The magma chamber is subject to a pressure drop of 10 MPa. As a result, the fault can be reactivated and slip in dip-slip and strike-slip motion. (B–D) Same as in Figure 2; the fault is shown only in D. Note that displacement vectors and fields are influenced by the fault.

(contours in Figure 2B) is influenced by the reactivated fault, with larger displacement vectors near the fault. The cross-sections show that evacuating the magma chamber results in higher horizontal (U_x) and vertical (U_z) displacements near the fault. The vertical displacement field U_z shows a maximum downward displacement centered above the chamber. Similarly, previous researchers have discussed the effect of freely slipping faults near magma chambers subject to pressure changes (Gargani et al., 2006). Some other studies considered circular faults around a magma chamber, as detailed below.

3.1.3. Deflating spherical magma chamber enclosed by a reactivated ring-fault

A caldera ring-fault can be considered a zone of weakness that may accumulate volcano-tectonic strain. In the end-member scenario, caldera ring-faults are free to slip, considerably affecting deformation at the surface. Figure 4 shows a circular fault at a radius of 10 km circumscribing the deflating magma chamber. The fault can be considered a ring-fault peripheral to the active magma system, and can be reactivated in dip-slip and strike-slip. All other model parameters are the same as described above. The horizontal displacement vectors show material convergence towards the reservoir (Figure 4B). In cross-section, the displacement U_x shows slightly smaller values near the surface (Figure 4C). In contrast, vertical displacement U_z shows a broad area of subsidence (Figure 4D). The bell-shaped area of peak subsidence is less expressed, meaning that subsidence would most likely occur as a uniform block, limited by the reactivated ring-fault. There is more subsidence than in models lacking such a ring-fault, although the pressure drop within the magma chamber is the same (cf. Figure 2). Several previous studies have considered the effect of reactivated ring-faults surrounding a magma chamber subject to pressure changes, for instance, at the caldera of Campi Flegrei, Italy. These studies analyze the extent of deformation due to magmatic or hydrothermal activity influenced by fault reactivation (Troise et al., 1997, 2003, 2004; Petrazzuoli et al., 1999; Beauducel et al., 2004). It must be noted that the pattern of displacement fields can vary depending on the type and geometry of the reactivated ring-fault.

3.2. Predicting the location of ring-dike intrusions

The following models consider an evacuating magma chamber and a passively opening ring-fault. Results are shown in map view and in side views, displaying the contoured amount of ring-fault opening. In these calculations, the displacement perpendicular to each element of the ring-fault is determined; a positive displacement means that ring-dike intrusion is facilitated, while a negative displacement signifies areas where ring-dike intrusions are hindered. These models are designed to predict the most likely location and direction of a ring-dike intrusion, based on the assumption that a ring-dike intrusion may preferentially occur where the ring-fault is opened.

Deflating spherical magma reservoir enclosed by reactivated ring-fault

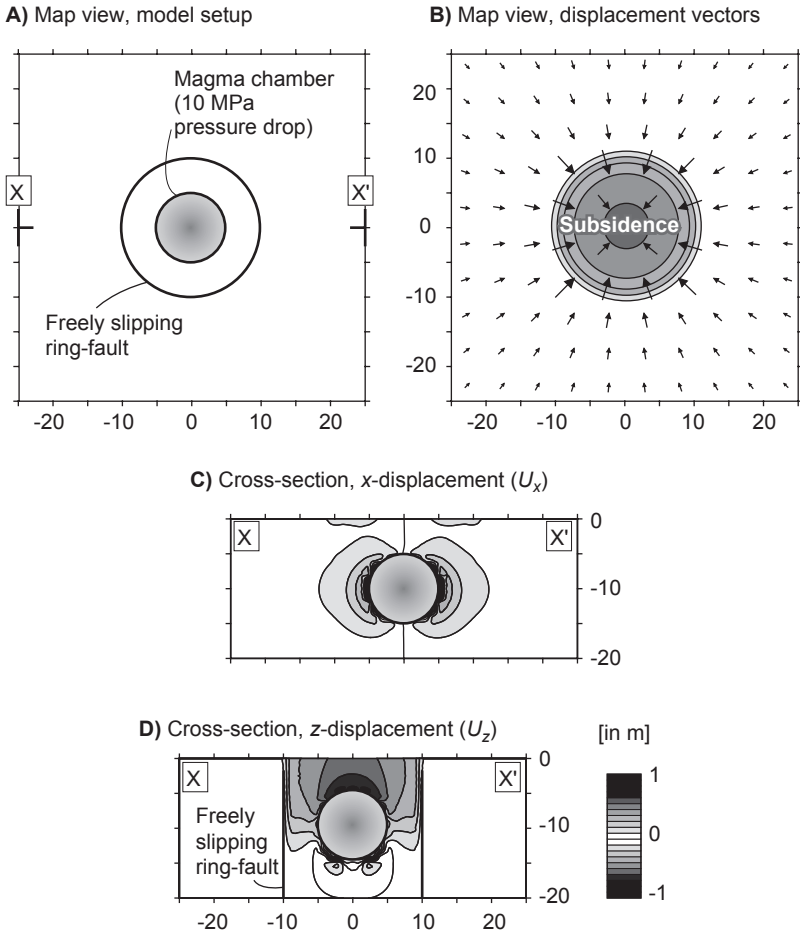


Figure 4 Deflation of a spherical magma chamber enclosed by a ring-fault. (A) Model setup (x – y plane). A ring-fault is defined surrounding the magma chamber, with a radius of 10 km at 2–20 km depth. The magma chamber is subject to a pressure drop of 10 MPa. As a result, the ring-fault may be reactivated and slip in dip-slip and strike-slip. (B)–(D) Same as in Figure 2. Displacement abruptly stops at the ring-fault, while U_z deformation is amplified inside the “caldera.”

3.2.1. Deflating spherical magma chamber

In this model, a deflating magma chamber is encircled by a ring-fault, which reaches from the base of the magma chamber to the surface (Figure 5). Displacement vectors and displacement contours suggest piston-type subsidence with the largest horizontal displacement in the periphery (Figure 5B). The side views onto the opening ring-dike (Figure 5C) show that the displacement at the ring-fault is largest at depth near the magma chamber and is radially uniform,

Deflating spherical magma reservoir, opening at ring-fault

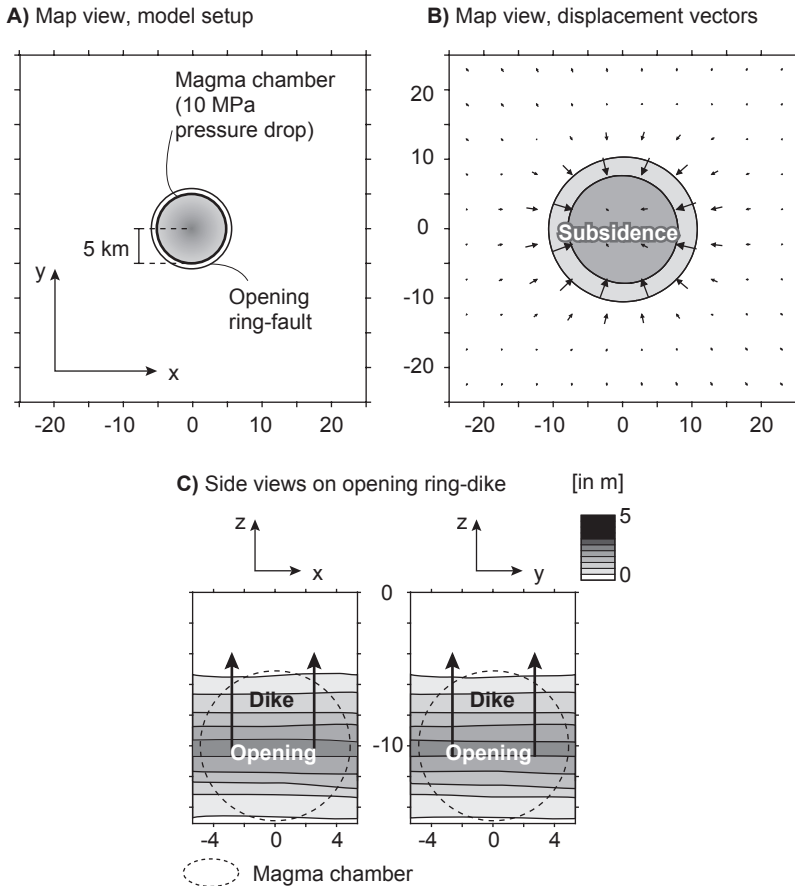


Figure 5 Deflation of a spherical magma chamber causes opening at a circumferential ring-fault. (A) Model setup (x - y plane). The magma chamber (5 km radius) is emplaced at (x , y) coordinates (0, 0) at 10 km depth, and is subject to a pressure drop of 10 MPa. A ring-fault is defined surrounding the magma chamber, with a radius of 5 km at 0–20 km depth. Boundary conditions are set so that the ring-fault is allowed to open. (B) A map view of horizontal displacement vectors at the surface (x - y plane) shows convergence toward the deflating source. Vector magnitudes are largest at the periphery and tend to become zero inside the caldera (piston subsidence). (C) Side views on opening ring-fault (left showing x - z plane, right y - z plane). The projection of the spherical magma chamber enclosed by the ring-fault in (C) is indicated as a dashed ring centered at 10 km depth. Maximum opening occurs near the magma chamber. The pattern is radially symmetric, so dike intrusion (shown by black arrow) may occur as a complete ring.

implying that a dike intrusion could occur anywhere along the ring-fault and in a complete circle around the magma chamber. Separate tests were done to study the effect of a ring-fault dipping in or out (not shown in figures), which affects the amount of opening in the sense that a larger amount of opening is found

for outwardly dipping ring-faults. However, a more complex shape of the ring-fault or magma chamber or a variably dipping ring-fault may yield variable amounts of opening, thus also affecting the geometry and completeness of a ring-dike.

3.2.2. Deflating sill-shaped magma chamber

Because magma chambers are typically flattened rather than spherical (Marsh, 2000), a sill-shaped (oblate spheroid) geometry must be considered, as it may significantly affect the distribution of ring-fault opening. In this model, a deflating sill-shaped magma chamber is encircled by a ring-fault, and the setup of the model is similar to the scenario described above with the only exception that the magma chamber is flat: 10 km wide and 5 km high (Figure 6). Depressurizing the sill-shaped magma chamber causes the most pronounced ring-fault opening along a narrow band around the magma chamber (Figure 6C). However, the amount of opening is smaller than for the spherical magma chamber model (note the different color scale in Figures 5 and 6). The most likely upward propagation path of a dike cannot be determined in this scenario, because the pressure source is perfectly radially symmetric; therefore, any location around the ring-fault may be used. This pattern significantly changes if the magma chamber is elliptical, as shown below.

3.2.3. Deflating an elliptical magma chamber

Most actual calderas and their associated ring-faults are not circular, but elliptical (Holohan et al., 2005). As a consequence, the pattern of ring-fault opening and intrusion differs significantly from the radially symmetric scenario. In this model, a sill-shaped deflating magma chamber elongated in the east-west direction is used (ellipsoid shaped). The magma chamber is 20 km long, 10 km wide, and 5 km high (elongated in the x -direction), and is encircled by a ring-fault (Figure 7A). The magma chamber center is 10 km below the surface and is subject to a pressure drop of 10 MPa (Figure 7B). The model predicts a maximum in ring-fault opening at magma chamber depths. The x - z and y - z side views onto the ring-fault show the regions subject to opening. The largest amount of opening occurs at the short-axis side of the elliptical ring-fault (Figure 7C left) and drops to zero along the long-axis side of the elliptical ring-fault (Figure 7C right). The model results can thus be interpreted in such a way that dike intrusions are more likely to occur and to propagate upward along the short-axis side of the elliptical ring-fault. It may also be possible that ring-dike intrusions change their intrusion direction and migrate laterally into the short-axis side, as indicated in Figure 7C. The caldera that formed the Bishop Tuff eruption at Long Valley, for instance, is thought to have initiated at the short-axis side, as suggested also by recent analog experiments (Holohan et al., in press).

Deflating sill-shaped magma reservoir, opening at ring-fault

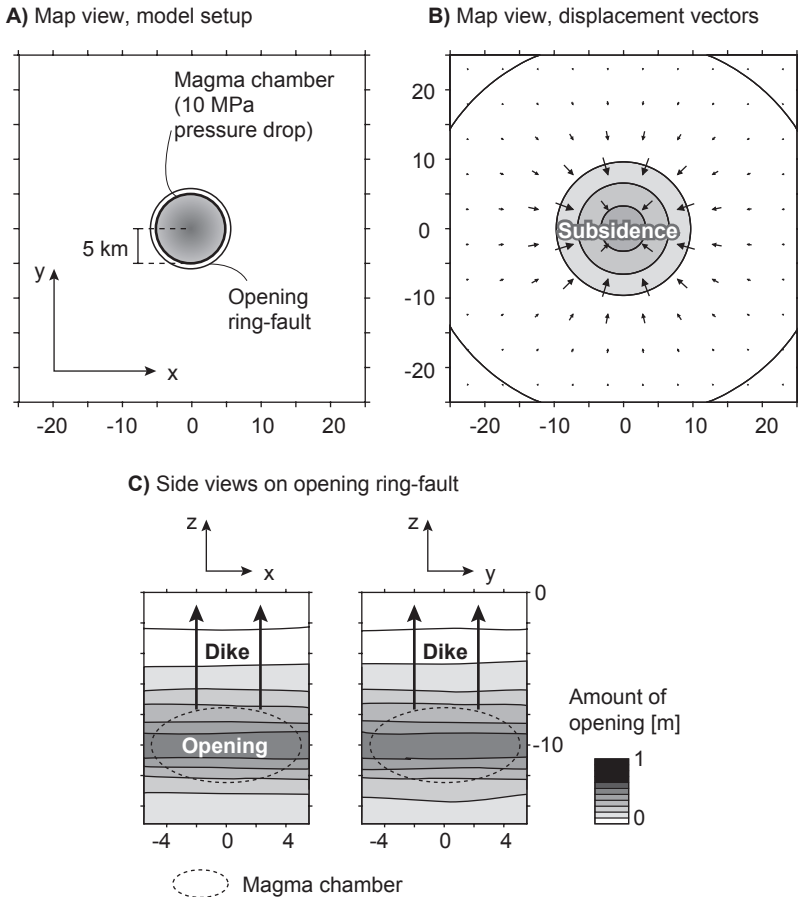


Figure 6 Deflation of a sill-shaped magma chamber causes opening at a circumferential ring-fault. The magma chamber is vertically flattened (5 km radius in x and y directions, 2.5 km in z direction, aspect ratio 2:1), emplaced at (x, y) coordinates $(0, 0)$ at 10 km depth, and is subject to a pressure drop of 10 MPa. All other parameters and subfigure explanations (A–C) are the same as in Figure 5. This model suggests that the zone of maximum opening is restricted to very close to the sill-shaped magma chamber. The pattern is radially symmetric, so dike intrusion (shown by black arrow) may occur as a complete ring.

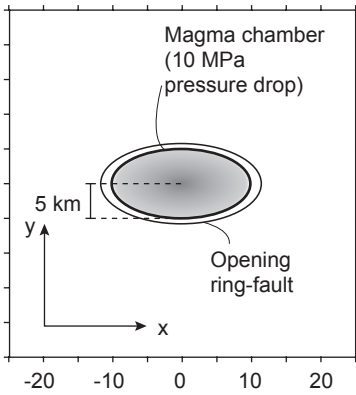
3.3. How processes external to the caldera system may affect the location of ring-dike intrusions

3.3.1. Tectonic earthquake at a distance

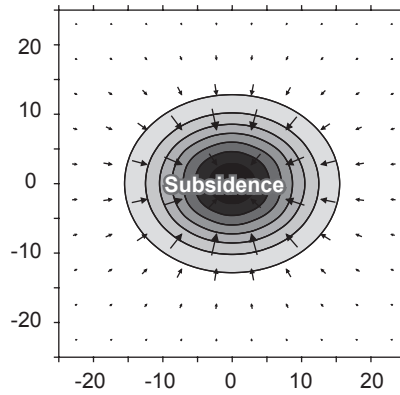
Many calderas systems are located in highly active tectonic regions where large earthquakes can occur and affect the activity of the volcano magma system. In this

Deflating elliptical magma reservoir, opening at ring-fault

A) Map view, model setup



B) Map view, displacement vectors



C) Side views on opening ring-fault, amount of opening

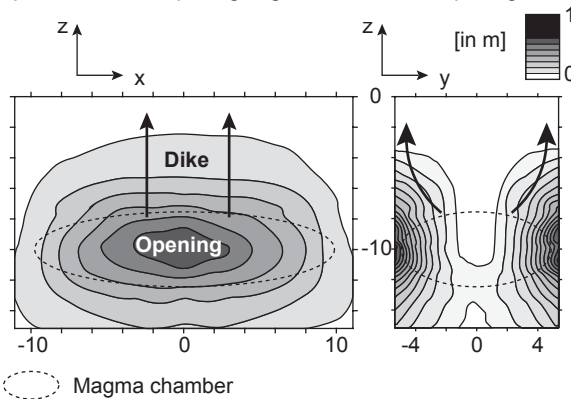
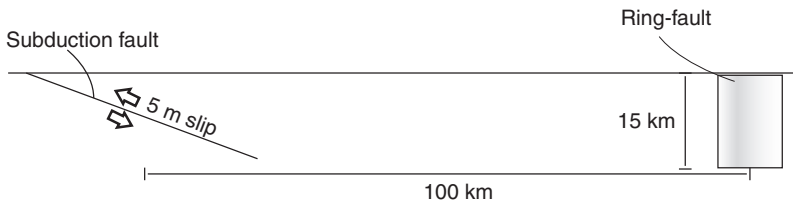


Figure 7 Deflation of an elliptical magma chamber causes opening at a circumferential ring fault. The magma chamber is elongated in the x -direction and vertically flattened (10 km radius in x , 5 km in y , and 2.5 km in z), emplaced at (x, y) coordinates (0, 0) at 10 km depth, and is subject to a pressure drop of 10 MPa. All other parameters and subfigure explanations (A–C) are the same as in Figure 5. The displacement parameters and subfigure explanations (A–C) are the same as in Figure 5. The displacement computed at the ring-fault suggests opening should occur at the short-axis side of the ring-fault. A potential dike intrusion would intrude as shown by the black arrow in (C).

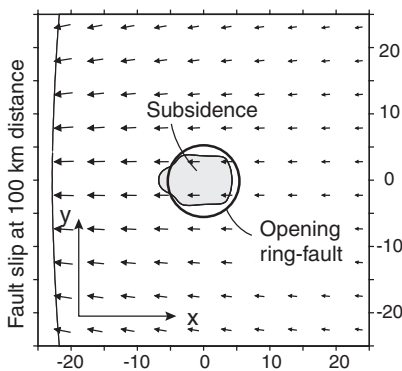
model, the effect of a tectonic earthquake distant from the ring-fault is considered. The earthquake is simulated by 5 m uniform slip on a 20×20 km fault, 100 km from the ring-fault (Figure 8A). A low-angle thrust earthquake is simulated, as if in a subduction zone. As in the models described above, the amount of opening is calculated at the ring-fault in order to predict the location of a ring-dike. Map view shows displacement vectors directed to the west towards the earthquake zone and slight subsidence due to the reactivated (opened) ring-fault (Figure 8B). The model predicts maximum opening at two opposite sides of the ring-fracture, with slightly

Tectonic earthquake at distance to ring-fault

A) Side view, model setup



B) Map view, displacement vectors



C) Side views on opening ring-fault

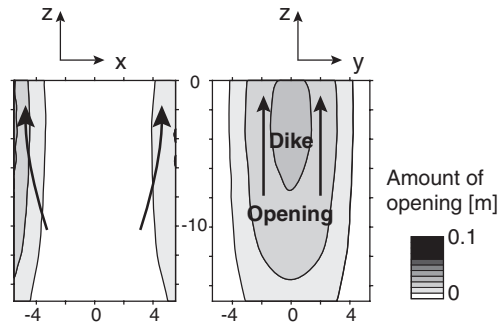


Figure 8 Remote tectonic deformation acting on a ring-fault. (A) Model setup (x - z plane). An earthquake was simulated 100 km from the ring-fault, its characteristics resembling a subduction earthquake. A ring-fault is defined with a radius of 5 km at 0–20 km depth. Boundary conditions are set so that the ring-fault is allowed to open due to the earthquake. (B) A map view of horizontal displacement vectors at the surface (x - y plane) shows displacement of the hanging wall toward the earthquake source. Note small subsidence caused by reactivation of the ring-fault. (C) Side views on opening ring-fault (left showing x - z plane, right showing y - z plane). Maximum opening occurs at two regions of the ring-fault. Dike intrusions into the ring-fault are encouraged perpendicular to the slip direction of the earthquake (potential dike paths shown by black arrow). A similar displacement pattern is expected for ring-faults subject to rifting episodes.

more on the side closer to the earthquake (Figure 8C). The model thus suggests that a dike intrusion is encouraged in these two zones, while complete ring-fault reactivation and ring-dike formation appears unlikely. A similar effect can be expected for zones subject to tectonic rifting. The models imply that tectonic deformation may have a large effect on the ring-dike intrusion pattern and thus also affect the location of an eruption.

3.3.2. Radial dike intrusion outside the ring-fault

Some systems are known for a pattern of radial dikes and fractures outside the caldera basin (e.g., Galapagos Islands, Chadwick and Howard, 1991; Gran Canaria,

Troll et al., 2002). In this model, an intrusion of a radial dike outside a caldera ring-fault is considered (Figure 9A). The radial dike is 15 km long and deep, and subject to 1 m of uniform opening. This induces a displacement at the adjacent ring-fault. Similar to the models described before, the ring-fault is allowed to open. The map-view displacement vectors show extension perpendicular to the dike and two lobes of uplift (Figure 9B), typical for shallow dike intrusions (Dzurisin, 2007). The side

Radial dike intrusion, opening at ring-fault

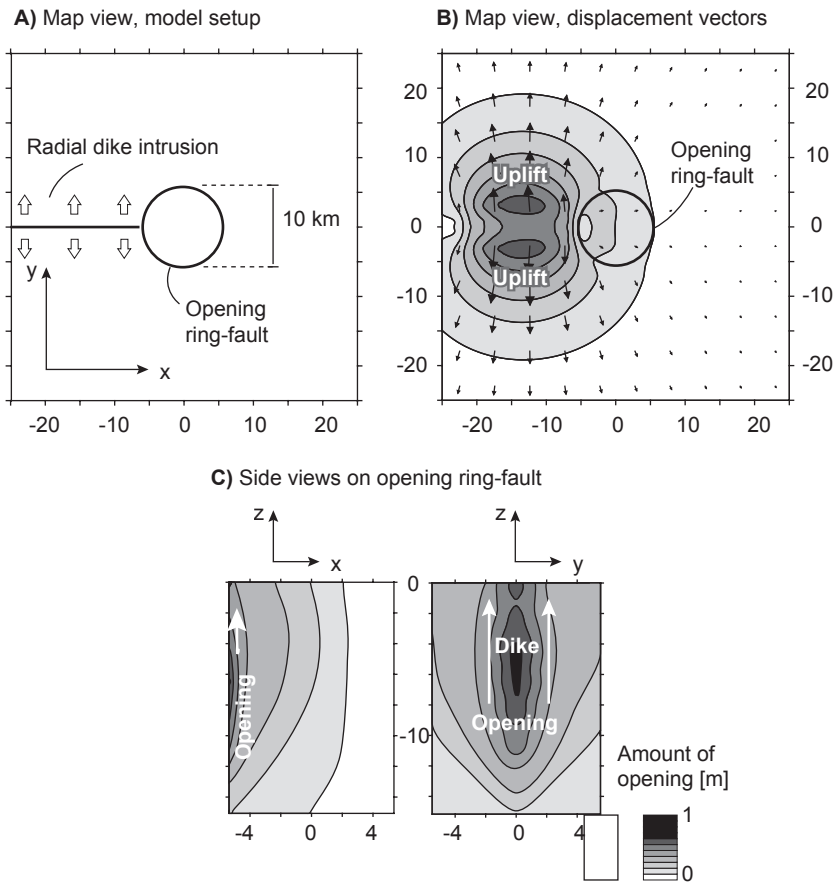


Figure 9 Radial dike intrusion causes opening of caldera ring-fault. (A) Model setup (x - y plane). A radial dike with an area of 15×15 km is subject to 1 m uniform opening. The dike is located outside a ring-fault. Boundary conditions are set so that the ring-fault is allowed to open. (B) A map view of horizontal displacement vectors at the surface (x - y plane) shows displacement perpendicular to the dike, with two lobes of maximum uplift in the periphery. U_z displacement contours are locally influenced by the opening ring-fault. (C) Side views shows opening of ring-fault (left shows x - z plane, right y - z plane) in the region facing the radial dike. The zones of opening can be more easily intruded by ring-dikes, so a radial dike may control the intrusion of an ensuing partial ring-dike.

views show that maximum opening occurs at the part of the ring-fault that is closest to the dike (Figure 9C). This suggests that ring-dike intrusion might occur at the segment of the ring-fault that is closest to the radial dike intrusion in the periphery of the caldera. Accordingly, a dipping dike would lead to ring-dike formation that obliquely propagates upwards.

4. DISCUSSION

This paper uses numerical models to (i) describe deformation around a depressurized magma chamber and test how local structures can affect this displacement, (ii) describe the potential of opening a ring-fault in order to examine the location at which potential dike intrusions occur, and (iii) describe how processes external to the caldera, such as an earthquake or radial intrusion, affect the location of a ring-dike intrusion.

The models are simplified and assume a homogeneous elastic material. Volcanoes, especially caldera volcanoes that experience a high degree of fracturing and hydrothermal weakening, may have a time-dependent viscoelastic rheology (Newman et al., 2001) and rock-strength values that vary by as much as several orders of magnitude (Watters et al., 2000). The variations in material may be lateral (due to fracturing, dikes, alteration) or vertical (due to lithologic layering, increasing confining pressure). Thus, the development of a stress field and the deformation pattern may be influenced by such heterogeneities (e.g., Manconi et al., 2007; Gudmundsson, 2006). One may speculate, for instance, that the amount of ground displacement in a deflating or inflating caldera basin can be amplified by rock types that have a lower modulus of elasticity. Likewise, the effect of external processes, such as earthquakes or dike intrusion in the periphery of the volcano, may have an effect on caldera systems. The models used in this study assume that the intrusion of ring-dikes as subvertical extensional fractures (mode I) is governed by opening perpendicular to a ring-fault. This generally agrees with historical caldera activity, where displacement often occurs along near-vertical ring-faults (Newhall and Dzurisin, 1988). However, it must be noted that this is a simplification of more complex geometries, as some historical caldera ring-faults have shear fractures that dip slightly inward (Darwin caldera) or outward (Rabaul caldera), the latter also approximating the findings of previous seminal work (Anderson, 1936, 1937). Some (probably most) dike intrusions intrude in a mixed-mode mechanism, including opening (mode I) but also strike-slip shear (mode II) and dip-slip shear (mode III) dislocation, which is not considered in the models presented here. Nevertheless, important conclusions can be drawn from these models, as shown by comparisons to natural caldera systems.

The models imply that a ring-dike forms in a uniform circular way only when the magma chamber is uniform, perfectly spherical, and not influenced by regional or external structures or deformation fields. Most other numerical models suggest that a potential ring-dike is more likely to intrude only partially into a ring-fault. Likewise, typical ring-dikes found in nature show such complexities, where in combination with the models summarized here, external influences can be assessed.

Surface eruptions circumscribing a caldera center have occurred at several locations, for instance, on Deception Island (1967–1969) and Niuafoou (1853, 1867) (Newhall and Dzurisin, 1988). While some historical caldera activity may have been related entirely to ring-dikes, others have been due to a dike that was partially reactivated and intruded a pre-existing fault. At Rabaul, a caldera system with a strongly elliptical outline, eruptive activity simultaneously occurred on opposite sides in 1878 and 1937 (Mori and McKee, 1987; Nairn et al., 1995; Saunders, 2004). At some caldera systems, ring-dike intrusions and eruptive activity occurred at two or more ring vents, as for example at the 20×30 km wide Tondano caldera in 1952 and 1971 (Lecuyer et al., 1997).

Several examples of calderas and their ring-dike structures are shown in Figure 10. The first image shows a downsag caldera, lacking prominent ring-fractures and ring-dikes. The Gross Brukkaros system in Namibia (Figure 10a) has not formed zones of major concentric structural weakness. The 10 km wide structure was first subject to shallow magma inflation at about 4 km depth (Komuro et al., 1984) and intense surface doming, bending the surface stratigraphy (Stachel et al., 1994). The doming phase was followed by depletion of up to 5 km^3 , but no major ring-dike or ring-fault structure was formed. This example illustrates that large magma evacuation and downsag caldera subsidence is possible without major structural fracturing and dike injection visible at the surface.

Intrusion around a caldera basin is the most comprehensible representation of a ring-dike. Some of the ring-dike intrusions occur along a single ring-fault, while others occur along several subparallel faults that form a near-concentric pattern at the surface. Ring-dikes are described in the Peninsular Range Batholiths of Baja California, Mexico, and southern California (Johnson et al., 2002). The formation of the Ramona ring-dike (Figure 10b) is thought to have been associated with a phase of subsidence of the caldera floor (Mirriam, 1941). Another elliptical ring structure is shown, from the El Pinal complex (Figure 10c), which is interpreted as a ring-dike that causes a well-developed contact zone (Duffield, 1968).

Ring-dike structures that develop in a region tectonically predisposed or subject to a tectonic stress field may develop very complex shapes. An intruding ring-dike may follow pre-existing faults or discontinuities and thus abruptly stop or change its direction, conditioned by various parameters such as material property, fault friction coefficient, pore pressure, and state of stress. A simple scenario was simulated here to illustrate the significance of pre-existing discontinuities. The numerical model showed that caldera subsidence close to a linear fault is highly asymmetrical, being focused at one side of the fault structure. The Erongo complex is one of the largest of the Damaraland complexes in Namibia, and shows a central 30 km wide massif with silicic intrusions, partly encircled by a tholeiitic ring-dike with a 50 km diameter (Figure 10d). The ring-dike half formed only on the north-western side of a SW–NE oriented regional fault that was thought to have been reactivated during intrusion (Wigand et al., 2004). It was suggested that the ring-dike formed after a caldera collapse (Wigand et al., 2004). The absence of a ring-dike on the segment opposing the fault implies that circular dike intrusion was hindered. The models shown in this study suggest that a reactivated tectonic fault may act as a barrier to deformation; so a change in magma chamber pressure leads to significant

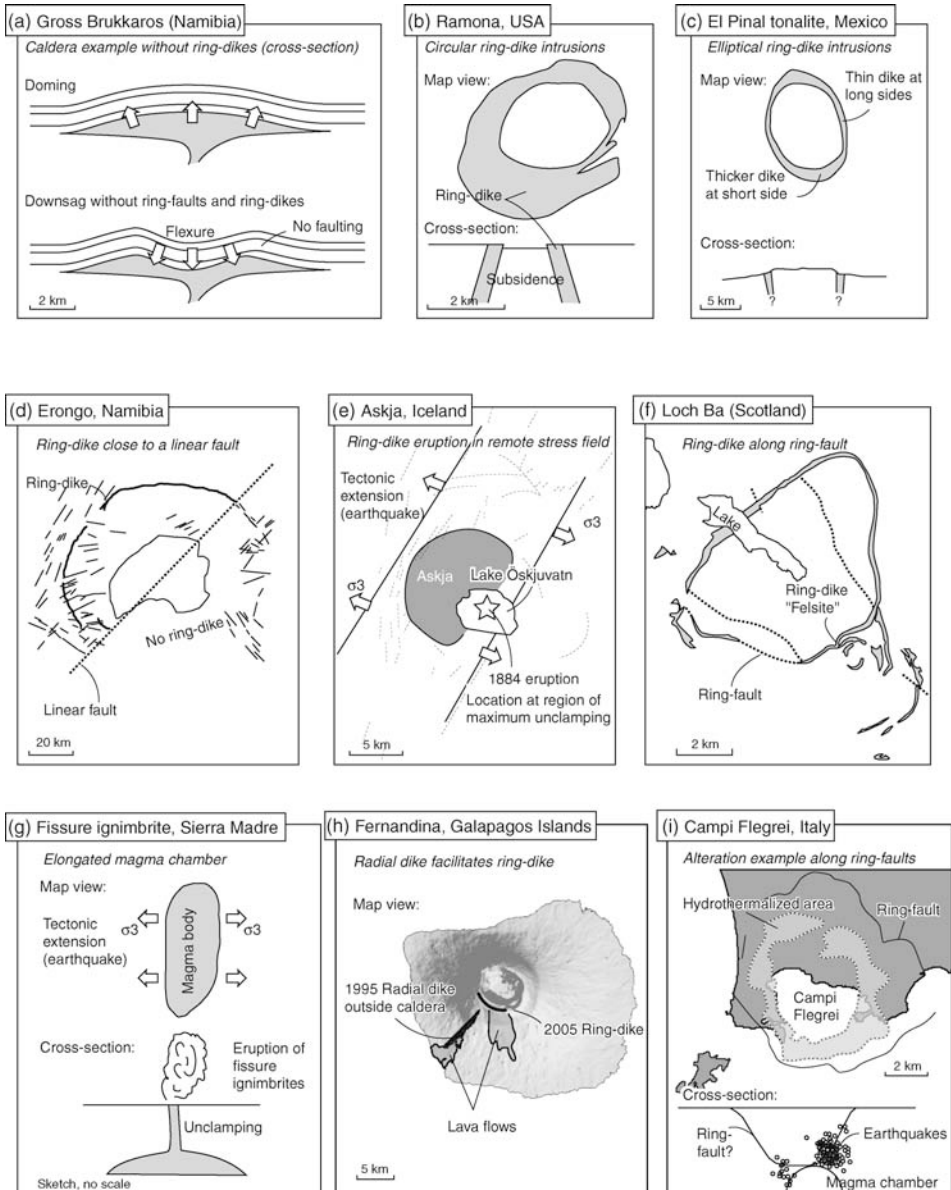


Figure 10 Examples of ring structures and ring-dikes. (a) After Stachel et al. (1994). (b) After Johnson et al. (2002). (c) After Johnson et al. (2002). (d) After Wigand et al. (2004). (e) After Sturkell and Sigmundsson (2000). (f) After Aguirre Diaz and Labarthe Hernandez (2003). (g) After Jonsson et al. (1999) and GVP (2005). (h) After Beauducel et al. (2004). (i) After (a). See discussion text for details.

deformation only on one side of the fault. Thus, dike intrusion occurs only on one part of the circle: the numerical models support the evolutionary hypothesis and structural development proposed for the Erongo complex (compare [Figures 3 and 4](#)).

Many caldera systems and ring-dikes form in areas that are subject to tectonic deformation. The Askja volcanic complex is located at the divergent plate boundary in northern Iceland and hosts the 8 km wide Askja caldera ([Sturkell and Sigmundsson, 2000](#)). In 1875, dike intrusion occurred in the south-eastern margin of the Askja caldera, associated with a Plinian eruption and a parasitic 4.5 km wide caldera that is now filled by Lake Öskjuvatn. The dike was part of a larger rifting event, and reactivated the south-eastern flank of the Askja caldera ring-fault. The models presented in this paper show that these parts of the ring-fault are subject to opening if a remote extensional deformation source is applied, for example, a tectonic earthquake or rifting. Dike opening due to tectonic extension is also proposed for large-scale eruptions in Mexico ([Aguirre Diaz and Labarthe Hernandez, 2003](#)). The so-called fissure ignimbrites are probably not directly related to caldera collapse, but may be related to tectonic unclamping of a main dike ([Figure 10g](#)).

A well-exposed ring-dike is known from Loch Ba at the igneous center of Mull, in northwestern Scotland ([Figure 10f](#)). Ring-dike emplacement occurred during the last major intrusive event of the volcanic center, intruded directly into a ring-fault. The dike is rhyolitic and contains up to 20% mafic inclusions, implying significant magma mixing ([Walker and Skelhorn, 1966](#); [Sparks, 1988](#)). The ring-dike is thought to have intruded the ring-fault during a rapid caldera collapse associated with the violent eruption of a welded tuff from a strongly zoned magma chamber ([Sparks, 1988](#)). The dike is mostly vertical and dips 70–80° outward in the north-western segment ([Bailey et al., 1924](#)). However, the ring-dike does not form a complete ring; instead, it intrudes with a variable thickness from 0 to 400 m along a ring 8 km in diameter. In areas where the dike did not intrude, a ring-fault is exposed. This suggests that the ring-dike intruded an existing ring-fault where variable opening of the ring-fault may be related to small variations in its orientation (strike and/or dip) or magma chamber geometry.

Volcanic activity outside of a caldera system may affect the location and timing of ring-dike intrusions. The Galapagos volcanoes are case examples for ring-dike intrusions that are surrounded by radial dikes in the periphery ([Chadwick and Howard, 1991](#)). Due to alternating radial and circumferential dikes, the Galapagos volcanoes developed a typical morphology, reminiscent of an “inverted soup bowl” ([Chadwick and Dieterich, 1995](#)). In 1995, a radial dike intrusion occurred on the south-west flank of Fernandina volcano ([Figure 10h](#), just outside of the 5 km-wide caldera ([Jonsson et al., 1999](#)). The volcano did not erupt until an eruptive dike intruded the ring-fault in the south-western part of the caldera in 2005. The 2005 dike is a ring-dike, and its location matches the location of maximum opening as suggested by the numerical models in this study (compare [Figure 9](#)).

The locations of ring-dike intrusions are probably consistent with areas of hydrothermal activity, alteration, and ore deposition ([Stix et al., 2003](#)). For the caldera of Campi Flegrei, uplift was suggested to be largely influenced by

reactivated ring-faults (Troise et al., 1997, 2003, 2004; Petrazzuoli et al., 1999; Beauducel et al., 2004; De Natale et al., 2006). In summary, the mechanical processes that reactivate ring-fractures by dikes may also be of major importance for hydrothermal activity that follows the same trend (Beauducel et al., 2004). Thus, understanding the formation and reactivation of ring-faults and their susceptibility to intruding ring-dikes is of major interest to earth scientists of various disciplines.

5. CONCLUSION

Periods of caldera unrest mainly reflect tectonic and magmatic processes. This paper focuses on potential intrusion patterns along caldera ring-faults. A systematic set of numerical models suggests that caldera deformation may be affected by pre-existing and reactivated tectonic faults and ring-fractures, and that sites of ring-dike intrusions are controlled by various tectonic and magmatic loading processes. A tectonic event like an earthquake may lead to localized displacements at caldera systems and affect the locations of ring-dike intrusions. The shape of a deflating magma chamber of ring-fault may also affect the locations of ring-dikes. In view of this the formation of complete ring-dikes appears to be difficult. Many natural calderas have ring-dikes that can be better understood by examining the local volcano-tectonic environment and considering the models summarized in this paper. The locations and patterns of ring-dike intrusions at caldera volcanoes can also be applied to the distribution of hydrothermal activity and ore deposition elsewhere.

ACKNOWLEDGEMENTS

This work benefited from numerous discussions at the International Workshop on Caldera Volcanism on Tenerife, organized by Joan Marti and Jo Gottsman. Constructive reviews by Brian O'Driscoll and Shigekazu Kusumoto are greatly appreciated. This work was financially supported by the Deutsche Forschungsgemeinschaft (DFG WA 1642/1-4).

REFERENCES

- Acocella, V., Cifelli, F., Fucicello, R., 2001. Analogue models of collapse calderas and resurgent domes. *J. Volcanol. Geotherm. Res.*, 104(1-4), 81-96.
- Aguirre Diaz, G.J., Labarthe Hernandez, G., 2003. Fissure ignimbrites: Fissure-source origin for voluminous ignimbrites of the Sierra Madre Occidental and its relationship with Basin and Range faulting. *Geology*, 31(9), 773-776.
- Anderson, E.M., 1936. The dynamics of the formation of cone sheets, ring dykes, and cauldron subsidence. *Proc. Indian Acad. Sci., Earth Planet. Sci.*, 56, 128-163.
- Anderson, E.M., 1937. Cone sheets and ring dikes: the dynamical explanation. *Bull. Volcanol.*, 2(1), 35-40.
- Bailey, E.M., Clough, C.T., Wright, W.B., Richey, J.E., Wilson, G.V., 1924. The tertiary and post-tertiary geology of Mull, Loch Aline, and Oban. *Mem. Geol. Surv. Scotland*, 1-445.

- Beauducel, F., De Natale, G., Obrizzo, F., Pingue, F., 2004. 3-D modelling of Campi Flegrei ground deformations: role of caldera boundary discontinuities. *Pure Appl. Geophys.*, 161(7), 1329–1344.
- Becker, A.A., 1992. *The Boundary Element Method in Engineering*. McGraw-Hill, New York, NY.
- Billings, M.P., 1943. Ring-dikes and their origin. *Trans N. Y. Acad. Sci., Series II*, 5, 131–144.
- Bonin, B., 1986. *Ring Complex Granites and Anorogenic Magmatism*. North Oxford Academic Publishers Ltd., London.
- Bosworth, W., Burke, K., Strecker, M., 2003. Effect of stress fields on magma chamber stability and the formation of collapse calderas. *Tectonics*, 22(4), 16–1–16–21.
- Burov, E.B., Guillou Frottier, L., 1999. Thermomechanical behavior of large ash flow calderas. *J. Geophys. Res.*, 104(10), 23081–23109.
- Chadwick, W.W., Jr., Dieterich, J.H., 1995. Mechanical modeling of circumferential and radial dike intrusion on Galapagos volcanoes. *J. Volcanol. Geotherm. Res.*, 66(1–4), 37–52.
- Chadwick, W.W., Jr., Howard, K.A., 1991. The pattern of circumferential and radial eruptive fissures on the volcanoes of Fernandina and Isabela islands, Galapagos. *Bull. Volcanol.*, 53(4), 259–275.
- Clough, C.T., Maufe, H.B., Bailey, E.B., 1909. The cauldron-subsidence of Glen Coe, and the associated igneous phenomena. *Q. J. Soc. Lond.*, 65, 611–678.
- Cole, J.W., Milner, D.M., Spinks, K.D., 2005. Calderas and caldera structures: a review. *Earth Sci. Rev.*, 69(1–2), 1–26.
- Comninou, M., Dundurs, J., 1975. The angular dislocations in a half space. *J. Elast.*, 5(3–4), 203–216.
- Crouch, S.L., Starfield, A.M., 1983. *Boundary Element Methods in Solid Mechanics*. George Allen and Unwin, London.
- De Natale, G., Troise, C., Pingue, F., Mastrolorenzo, G., Pappalardo, L., Battaglia, M., Boschi, E., 2006. The Campi Flegrei Caldera: unrest mechanisms and hazards. In: Troise, C., De Natale, G., Kilburn, C. (Eds), *Mechanisms of Activity and Unrest at Large Calderas*. Geological Society, London Special Publications, Vol. 269, pp. 25–45.
- Druitt, T.H., Sparks, R.S.J., 1984. On the formation of calderas during ignimbrite eruptions. *Nature*, 310(5979), 679–681.
- Duffield, W., 1968. The petrology and structure of the El Pinal tonalite, Baja California, Mexico. *Geol. Soc. Am. Bull.*, 79, 1351–1374.
- Dzurisin, D., 2007. *Volcano Deformation*. Springer, Chichester.
- Gargani, J., Geoffrey, L., Gac, S., Cravoisier, S., 2006. Fault slip and Coulomb stress variations around a pressured magma reservoir: consequences on seismicity and magma intrusion. *Terra Nova*, 18, 403–411.
- Geyer, A., Folch, A., Marti, J., 2006. Relationship between caldera collapse and magma chamber withdrawal: an experimental approach. *J. Volcanol. Geotherm. Res.*, 157(4), 375–386.
- Gudmundsson, A., 1988. Formation of collapse calderas. *Geology*, 16(9), 808–810.
- Gudmundsson, A., 1998. Formation and development of normal-fault calderas and the initiation of large explosive eruptions. *Bull. Volcanol.*, 60(3), 160–170.
- Gudmundsson, A., 1999. Explosive eruptions triggered by dip-slip on caldera faults. *Volcanol. Seismol.*, 20(2), 239–254.
- Gudmundsson, A., 2006. How local stresses control magma-chamber ruptures, dyke injections, and eruptions in composite volcanoes. *Earth-Sci. Rev.*, 79(1–2), doi: 10.1016/j.earscirev.2006.06.006.
- GVP, 2005. Global Volcanism Program. Smithsonian Institution, <http://www.volcano.si.edu/>
- Holohan, E.P., Troll, V.R., van Wýk de Vries, B., Walsh, J.J., Walter, T.R., in press. Unzipping Long Valley: an explanation for vent migration patterns during an elliptical ring-fracture eruption. *Geology* G24329AR.
- Holohan, E.P., Troll, V.R., Walter, T.R., Muenn, S., McDonnell, S., Shipton, Z.K., 2005. Elliptical calderas in active tectonic settings: an experimental approach. *J. Volcanol. Geotherm. Res.*, 144(1–4), 119–136.
- Johnson, S.E., Schmidt, K.L., Tate, M.C., 2002. Ring complexes in the Peninsular Ranges Batholith, Mexico and the USA: magma plumbing systems in the middle and upper crust. *Lithos*, 61(3–4), 187–208.

- Jonsson, S., Zebker, H., Cervelli, P., Segall, P., Garbeil, H., Mougini Mark, P., Rowland, S., 1999. A shallow-dipping dike fed the 1995 flank eruption at Fernandina volcano, Galapagos, observed by satellite radar interferometry. *Geophys. Res. Lett.*, 26(8), 1077–1080.
- Kennedy, B., Stix, J., 2003. Igneous rock associations of Canada 2. Stages in the temporal evolution of calderas. *Geosci. Canada*, 30(3), 129–140.
- Kennedy, B., Stix, J., 2007. Magmatic processes associated with caldera collapse at Ossipee ring dyke, New Hampshire. *Geol. Soc. Am. Bull.*, 119(1), 3–17.
- Komuro, H., 1987. Experiments on cauldron formation: a polygonal cauldron and ring fractures. *J. Volcanol. Geotherm. Res.*, 31(1–2), 139–149.
- Komuro, H., Fujita, Y., Kodama, K., 1984. Numerical and experimental models on the formation mechanism of collapse basins during the Green Tuff orogenesis of Japan. *Bull. Volcanol.*, 47, 649–666.
- Kusumoto, S., Takemura, K., 2003. Numerical simulation of caldera formation due to collapse of a magma chamber. *Geophys. Res. Lett.*, 30(24), 2278, doi:10.1029/2003GL018380.
- Kusumoto, S., Takemura, K., 2005. Caldera geometry determined by the depth of the magma chamber. *Earth Planets Space*, 57(12), 17–20.
- Lecuyer, F., Bellier, O., Gourgaud, A., Vincent, P.M., 1997. Tectonique active du Nord-Est de Sulawesi (Indonésie) et contrôle structural de la caldeira de Tondano. *C.R. Acad. Sci. Paris*, 325(8), 607–613.
- Lipman, P.W., 1984. The roots of ash flow calderas in western North America: windows into the tops of granitic batholiths. *J. Geophys. Res.*, 89(B10), 8801–8841.
- Lipman, P.W., 1997. Subsidence of ash-flow calderas: relation to caldera size and magma-chamber geometry. *Bull. Volcanol.*, 59(3), 198–218.
- Manconi, A., Walter, T.R., Amelung, F., 2007. Effects of mechanical layering on volcano deformation. *Geophys. J. Int.*, 170(2), 952–958.
- Marsh, B.D., 2000. Magma chambers. In: *Encyclopedia of Volcanoes 1*. Academic Press, San Diego, CA, pp. 191–206.
- Marti, J., Folch, A., Neri, A., Macedonio, G., 2000. Pressure evolution during explosive caldera-forming eruptions. *Earth Planet. Sci. Lett.*, 175(3–4), 275–287.
- Marti, J., Vila, J., Rey, J., 1996. Deception Island (Bransfield Strait, Antarctica): an example of a volcanic caldera developed by extensional tectonics. In: McGuire, W.J., Jones, A.P. Neuberger, J. (Eds), *Volcano Instability on the Earth and Other Planets*, Geological Society, London Special Publications, Vol. 110, pp. 253–265.
- Mirriam, R.H., 1941. A southern California ring-dike. *Am. J. Sci.*, 239, 365–371.
- Mori, J., McKee, C.O., 1987. Outward-dipping ring-fault structure at Rabaul caldera as shown by earthquake locations. *Science*, 235(4785), 193–195.
- Nairn, I.A., McKee, C.O., Talai, B., Wood, C.P., 1995. Geology and eruptive history of the Rabaul caldera area, Papua New Guinea. *J. Volcanol. Geotherm. Res.*, 69(3–4), 255–284.
- Newhall, C.G., Dzurisin, D., 1988. Historical unrest at large calderas of the world. *US Geological Survey*, Reston, VA, 1108 pp.
- Newman, A.V., Dixon, T.H., Ofoegbu, G.I., Dixon, J.E., 2001. Geodetic and seismic constraints on recent activity at Long Valley caldera, California: evidence for viscoelastic rheology. *J. Volcanol. Geotherm. Res.*, 105(3), 183–206.
- O'Driscoll, B., Troll, V.R., Reavy, R.J., Turner, P., 2006. The great eucrite intrusion of Ardnamurchan, Scotland: reevaluating the ring-dike concept. *Geology*, 34(3), 189–192.
- Petrazzuoli, S.M., Troise, C., Pingue, F., De Natale, G., 1999. The mechanics of Campi Flegrei unrests as related to plastic behaviour of the caldera borders. *Annali di Geofisica*, 42(3), 529–544.
- Pinel, V., Jaupart, C., 2005. Caldera formation by magma withdrawal from a reservoir beneath a volcanic edifice. *Earth Planet. Sci. Lett.*, 230(3–4), 273–287.
- Richey, J.E., 1935. *British Regional Geology. Scotland: The Tertiary Volcanic Districts*. Edinburgh: HMSO for the Department of Scientific and Industrial Research Geological Survey and Museum, 1st edition. 8vo. vii[i], 115pp.

- Roche, O., Druitt, T.H., Merle, O., 2000. Experimental study of caldera formation. *J. Geophys. Res.*, 105(1), 395–416.
- Saunders, S.J., 2004. The possible contribution of circumferential fault intrusion to caldera resurgence. *Bull. Volcanol.*, 67(1), 57–71.
- Smith, R.L., Bailey, R.A., 1968. Resurgent cauldrons. In: *Studies in Volcanology*. Geological Society of America (GSA), Boulder, CO, pp. 613–662.
- Sparks, R.S.J., 1988. Petrology and geochemistry of the Loch Ba ring-dyke, Mull (N.W. Scotland): an example of the extreme differentiation of tholeiitic magmas. *Contrib. Min. Petrol.*, 100(4), 446–461.
- Sparks, R.S.J., Huppert, H.E., Turner, J.S., 1984. The fluid dynamics of evolving magma chambers. *Philos. Trans. R. Soc. Lond.*, 310(1514), 511–534.
- Stachel, T., Brey, G., Stanistreet, I.G., 1994. Gross Brukkaros — the unusual intracaldera sediments and their magmatic components. *Commun. Geol. Surv. Namibia*, 9, 23–41.
- Stix, J., Kennedy, B., Hannington, M., Gibson, H., Fiske, R., Mueller, W., Franklin, J., 2003. Caldera-forming processes and the origin of submarine volcanogenic massive sulfide deposits. *Geology*, 31(4), 375–378.
- Sturkell, E., Sigmundsson, F., 2000. Continuous deflation of the Askja caldera, Iceland, during the 1983–1998 noneruptive period. *J. Geophys. Res.*, 105(11), 25671–25684.
- Thomas, A.L., 1993. Poly3D: a three-dimensional, polygonal element, displacement discontinuity boundary element computer program with applications to fractures, faults, and cavities in the earth's crust. M.S. Thesis, Stanford University, Stanford, CA, pp. 1–221.
- Troise, C., De Natale, G., Pingue, F., 2004. Non-linear effects in ground deformation at calderas due to the presence of structural discontinuities. *Ann. Geophys.*, 47(4), 1513–1520.
- Troise, C., De Natale, G., Pingue, F., Zollo, A., 1997. A model for earthquake generation during unrest episodes at Campi Flegrei and Rabaul calderas. *Geophys. Res. Lett.*, 24(13), 1575–1578.
- Troise, C., Pingue, F., De Natale, G., 2003. Coulomb stress changes at calderas: modeling the seismicity of Campi Flegrei (southern Italy). *J. Geophys. Res.*, 108(6), 2292, doi:10.1029/2002JB002006.
- Troll, V.R., Walter, T.R., Schmincke, H.U., 2002. Cyclic caldera collapse: piston or piecemeal subsidence? Field and experimental evidence. *Geology*, 30(2), 135–138.
- Turcotte, D.L., Schubert, G., 2002. *Geodynamics*, 2nd edn. Cambridge University Press, Cambridge.
- Walker, G.P.L., 1984. Downsag calderas, ring faults, caldera sizes, and incremental caldera growth. *J. Geophys. Res.*, 89(B10), 8407–8416.
- Walker, G.P.L., Skelhorn, R.R., 1966. Some associations of acid and basic igneous rocks. *Earth Sci. Rev.*, 2(2), 93–109.
- Walter, T.R., Acocella, V., Neri, M., Amelung, F., 2005. Feedback processes between magmatic events and flank movement at Mount Etna (Italy) during the 2002–2003 eruption. *J. Geophys. Res.*, 110(B10205), 1–12.
- Walter, T.R., Amelung, F., 2006. Volcano–earthquake interaction at Mauna Loa volcano, Hawaii. *J. Geophys. Res.*, 111(B05204), 1–17. doi:10.1029/2005JB003861.
- Walter, T.R., Troll, V.R., 2001. Formation of caldera periphery faults: an experimental study. *Bull. Volcanol.*, 63(2–3), 191–203.
- Watters, R.J., Zimelman, D.R., Bowman, S.D., Crowley, J.K., 2000. Rock mass strength assessment and significance to edifice stability, Mount Rainier and Mount Hood, Cascade Range volcanoes. *Pure Appl. Geophys.*, 157(6–8), 957–976.
- Wigand, M., Schmitt, A.K., Trumbull, R.B., Villa, I.M., Emmermann, R., 2004. Short-lived magmatic activity in an anorogenic subvolcanic complex: $^{40}\text{Ar}/^{39}\text{Ar}$ and ion microprobe U–Pb zircon dating of the Erongo, Damaraland, Namibia. *J. Volcanol. Geotherm. Res.*, 130(3–4), 285–305.
- Yang, X.M., Davis, P.M., Dieterich, J.H., 1988. Deformation from inflation of a dipping finite prolate spheroid in an elastic half-space as a model for volcanic stressing. *J. Geophys. Res.*, 93(5), 4249–4257.